COMPEL - The international journal for computation and mathematics in electrical and electronic engineering

Electric field distribution during electroporation process in presence of nanoparticles

Caterina Bernardini
Department of Industrial Engineering, University of Padova, Padova, Italy

Elisabetta Sieni
Department of Pure and Applied Sciences, University of Insubria, Varese, Italy

Patrizia Lamberti
Department of Information and Electrical Engineering and Applied Mathematics, University of Salerno, Fisciano, Italy

Maria Evelina Mognaschi and Paolo Di Barba
Department of Electrical, Computer and Biomedical Engineering, University of Pavia, Pavia, Italy

Fabrizio Dughiero
Department of Industrial Engineering, University of Padova, Padova, Italy, and

Vincenzo Tucci
Department of Information and Electrical Engineering and Applied Mathematics, University of Salerno, Fisciano, Italy

Received 10 April 2026
Revised 25 June 2026
Accepted 27 June 2026

Abstract

Purpose – This study aims to present a numerical model to predict the electric field distribution in the presence of conductive or dielectric nanoparticles close to the cell membrane during electrochemotherapy treatment.

Design/methodology/approach – To solve the electromagnetic problem in transient conditions, finite element analyses are performed. Specifically, the field distribution during both the rise and the constant period of the pulse is investigated. To analyze the impact of the pulse dynamics, different rise times are considered.

Findings – The effect of a trapezoidal voltage pulse on the electric field distribution in a region of interest close to the nanoparticle is studied, considering nanoparticles made of conductive or dielectric materials.

Funding: Work partially supported by the European Union's Horizon Europe research and innovation program under the Marie Skłodowska Curie grant agreement No 101086142 (FLORIN project) and by the Italian National Recovery and Resilience Plan (NRRP) of NextGenerationEU, Mission 4, Component 2, Investment 1.1, Call for tender No. 1409 of 14.9.2022 of the Italian Ministry of University and Research (MUR), Project Title DEEPEST (Digging into rEversible and irreversible ElectroPoration: in vitro and in silico multiphysical analyses on cEll modelS for cancer Treatment) CUP B53D23002500006 – Grant Assignment Decree No. 960 of 30/06/2023.

COMPEL - The international journal for computation and mathematics in electrical and electronic engineering
Emerald Publishing Limited
0332-1649
DOI 10.1108/COMPEL-04-2026-0201

Originality/value – The effect of different nanoparticle materials is studied, as well as the effect of the pulse rise time.

Keywords Finite element analysis, Electroporation, Electric field, Nanoparticles, Nanotechnology

Paper type Research paper

1. Introduction

Electroporation is used to improve cell membrane permeability using a voltage pulse to generate a local electric field to open holes and improve drug uptake (Gehl, 2003; Mir, 2001). It is well known that the electric field distribution depends on the electric properties of the material (Campana *et al.*, 2018; Denzi *et al.*, 2015; Kranjc and Miklavčič, 2016). Numerical models were used to investigate on a tissue scale (Corovic *et al.*, 2013; Poignard *et al.*, 2016) the effect of the presence of nanoparticles (NPs) in the system adopted for inducing the cell electroporation. To study the influence of NPs, the electromagnetic problem has to be studied at cell level, as in Guo *et al.* (2024) and Krassowska and Filev (2007). Lekner in Lekner (2014) theorized the influence of conductive NPs in electroporation application, evidencing that such NPs could enhance electroporation. The present study is conducted by means of numerical simulations to study the electric field distribution in the presence of NPs made of different materials. In fact, a different distribution of the electric field is expected if dielectric or conductive NPs are close to the cell membrane due to the difference in the electric properties of the materials.

In Chiaramello *et al.* (2021a), the effect of gold NPs has been studied. The problem was verified experimentally in Ghorbel *et al.* (2019), where an improvement of electroporation using conductive NPs is obtained. Nevertheless, some authors disagree with this thesis, as in Polajžer *et al.* (2025), where some formulations of Au NPs do not lead to an electroporation improvement. From the literature, no clear indications can be obtained concerning the role of the electric nature (conductive vs insulating) of the NP neighboring the cell in electroporation enhancement.

In this paper, the electric field distribution around the cell membrane in the presence of elongated NPs made of conductive or dielectric material is investigated. Moreover, the effects of the orientation of the NP with respect to a hypothesized spherical cell are studied. The gold NP with an elongated shape is the one studied by Lekner in Lekner (2014). To solve the electromagnetic problem and compute the electric field strength, among the different possible numerical approaches proposed in the literature (see, e.g. Sel *et al.*, 2005), a dynamic current distribution problem is proposed in this paper, similar to the one suggested in Sieni *et al.* (2023). The analysis of the electric field distribution with and without NP gives information about the impact of the NP in proximity to the cell membrane, evaluated as a variation of the intensity of the electric field. The idea is to analyze the effect of a NP on the electric field distribution close to the cell membrane during the transient part of the voltage pulse. In particular, we have computed the electric field due to a trapezoidal voltage pulse with a predefined rise time applied to the system at two time instants, one belonging to the rise-time interval and a second one belonging to the part of the pulse where the voltage is constant. In this way, the transient effect during the pulse increment from 0 V to the plateau voltage is studied. Hence, the electromagnetic problem is solved during the transient, focusing on the rise-time interval. The electric field distribution in a region-of-interest (ROI) close to the cell membrane is evaluated and compared to the distribution obtained with a constant value of the voltage, i.e. solving a static conduction problem. Two different values of rise time of the trapezoidal voltage pulse are considered to investigate the electric field distribution in the ROI.

2. The finite element model

Figure 1(a) shows the two-dimensional geometry of a cell with cytosol and membrane, diameter of 20 μm and membrane thickness 7 nm. The cell is immersed in a 1 × 1 mm square domain representing the extracellular matrix made of cell culture medium. The two electrodes are supplied by a voltage pulse, as shown in Figure 1(b). This configuration of a cell between a couple of electrodes is a typical model proposed in the literature by different authors, for example, Chiaramello *et al.* (2021b), Guo *et al.* (2024), P. Lamberti *et al.* (2013) and Sieni *et al.* (2023).

Close to the cell membrane, a single NP shaped like a rod of size 500 × 100 nm is positioned. The NP geometry includes an external layer 7 nm thick. The applied voltage is a symmetric trapezoidal pulse 100 μs long, magnitude 50 V and a rise time from 1 to 10 μs. The voltage pulse length is typical of the standard protocols of an electrochemotherapy treatment (Gehl *et al.*, 2018). The rise time of the voltage pulse is in accordance with that of typical generators used in the laboratory (Bertacchini, 2017; IGEA, 2026). In this case, at pulse plateau, an electric field strength of 500 V/cm was applied. This electric field strength corresponds to the minimum electric field for some type of cell to start electroporation (Mir, 2006; Mir *et al.*, 2006). This value has been chosen to verify the NPs effect in terms of local enhancement of the electric field. The electrical properties of the materials used in the models are summarized in Table 1. Both electric conductivity σ, and dielectric permittivity ε are assumed to be linear, homogeneous and isotropic properties.

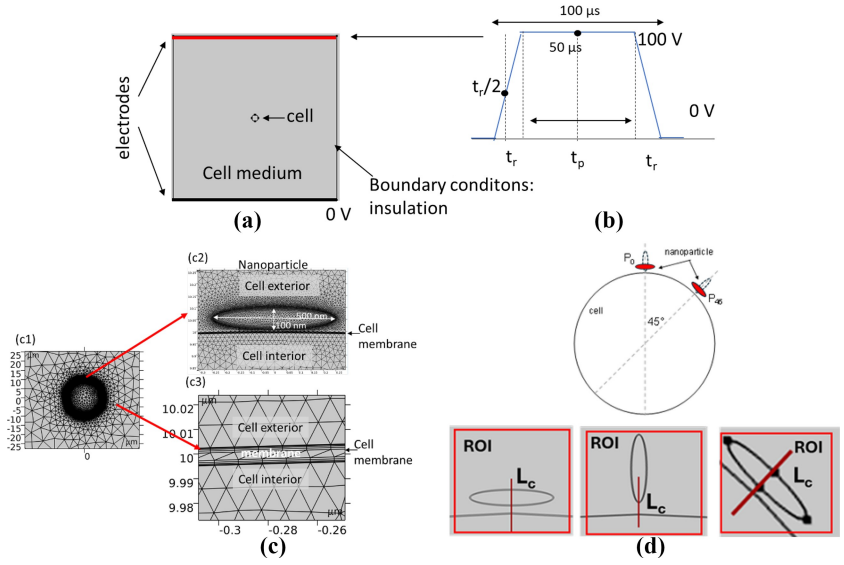

Figure 1. (a) Geometry of the simulated model and (b) time evolution of the applied voltage pulse. (c) Mesh of (c1) the geometry with details at the (c2) boundary between the nanoparticle and the cell, and (c3) in the membrane region. (d) Position of nanoparticle close to the cell membrane. Zoom of geometry for a (left) horizontal, (center) vertical and at 45° (right) nanoparticle. Sample line Lc and ROI (red rectangle)

Source: Authors' own work

COMPEL

The problem geometry in Figure 1 was solved as an electric field problem by means of finite element analysis (FEA) (Meunier, 2008). The mesh, whose detail is shown in Figure 1(c), has approximately 290,000 triangular elements, whereas the ROI has approximately 95,000 elements. In the cell membrane, a layered mesh was designed and represented in Figure 1(c). This mesh guided the mesh in the area close to the cell membrane and NP. The same strategy was used in the external layer of the NP.

Because of the material properties (i.e. permittivity and conductivity, Table 1) and the time scale of the applied pulse in the order of microseconds, an electro-quasi-static formulation is solved (Haus and Melcher, 1989). It is a diffusion problem, where both conduction and displacement currents are considered while the electromagnetic induction is neglected:

$$\nabla \cdot \left(\sigma \nabla V + \varepsilon \frac{\partial}{\partial t} \nabla V \right) = 0 \tag{1}$$

where V is the scalar electric potential subject to appropriate boundary conditions and initial conditions. Specifically, at the electrodes, the Dirichlet conditions are forced, while Neumann conditions hold on the external boundary. Initial conditions correspond to zero field in the whole domain.

A posteriori, the electric field $\mathbf{E} = -\nabla V$ is uniquely derived thanks to the assumption of the irrotational field.

It can be noted that the two terms in equation (1) take into account the effect of drift and diffusion, respectively, in charge transportation. Therefore, they can be described as equivalent current densities, specifically conduction current density $\mathbf{J}_c = \sigma \nabla V$ and displacement current density $\mathbf{J}_d = \varepsilon \frac{\partial}{\partial t} \nabla V$.

Equation (1) is solved using the Comsol Multyphysics AC/DC module (www.comsol.com, COMSOL AB, Stockholm, Sweden). In particular, the conduction current module with a time-transient solution was used. In COMSOL, when the electric current module is used in time-dependent studies, the current density also includes the displacement current dD/dt. Any magnetic material is used in this problem, but the model used takes into account both conduction and dielectric current components as well as the transient effect related to pulse rise time. The current density components associated with conduction and displacement were evaluated in the entire domain and in the membrane domain. The electric field strength is sampled on the lines Lc in Figure 3 inside the ROI marked with the red rectangle, approximately sized 1,500 × 1,500 nm^2.

Table 1. Electric properties of the materials; [NU] = not unit

Model domain	Electrical conductivity σ [S m^{-1}]	Relative permittivity εr [NU]	References
Cytosol	0.13	60	(Zudans *et al.*, 2007)
Membrane	5.3 10^{-6}	12.8	(Goldberg *et al.*, 2018; Lamberti *et al.*, 2015; Pavlin *et al.*, 2005)
Culture medium	1.3	80	(Ivorra *et al.*, 2010; Pavlin *et al.*, 2005; Pucihar *et al.*, 2001)
Au NP	4.1 10^{7}	10	(Gauthier, 1995; Zu *et al.*, 2014).
Silica NP	10^{-13}	3	(Ferry and Rode, 2025; "Properties", 2026)

Material properties used in simulations are summarized in Table 1 and are taken from the literature. In particular, it was considered that cytoplasm conductivity depends on the cell type and it ranges between 0.02 and 1 S/m (Labeed *et al.*, 2006; Wang *et al.*, 2017; Zhao *et al.*, 2014) and relative permittivity $\varepsilon_r = \varepsilon/\varepsilon_0$, where $\varepsilon_0 = 8.854\ 10^{-12}$ F/m is the absolute permittivity of the free space between 80 and 150 (Goldberg *et al.*, 2018; Guo *et al.*, 2022; Ye *et al.*, 2010). Zudans reported a cytoplasm conductivity of 0.13 S/m (Zudans *et al.*, 2007). Instead, the membrane conductivity has typical values in the order of $10^{-6} - 10^{-7}$ S/m; the relative permittivity is close to 10 (Goldberg *et al.*, 2018; Lamberti *et al.*, 2015; Pavlin *et al.*, 2005). Culture media depend on the specific type and can range from low conductivity to high conductivity, typically 0.2 S/m or between 1 and 1.5 S/m, with a typical relative permittivity of 80 (Ivorra *et al.*, 2010; Pavlin *et al.*, 2005; Pucihar *et al.*, 2001). Finally, the electrical properties of NPs have been selected according to the data reported in Ferry and Rode (2025), Gauthier (1995), "AZoM", (2026) and Zu *et al.* (2014).

3. Results

3.1 Field patterns in time

It is interesting to show the field pattern associated with $\mathbf{J}_c$ and $\mathbf{J}_d$ at selected time instants. Figure 1(d) shows the magnitude of the conduction, $|\mathbf{J}_c|$, and displacement, $|\mathbf{J}_d|$, components of the current density, excited by an electric pulse with a rise time of 10 μs. The patterns are shown at different time instants, considering only the cell without NPs, in an 80×80 μm square. In particular, the following time instants have been considered: 1, 5, 10, 11 and 50 μs. It can be noted that the conduction current density [upper line in Figure 1(d)] increases until the pulse plateau and reaches its maximum strength at the plateau. In contrast, the displacement current density [middle line in Figure 1(d)] is larger during the pulse rise time (at 1, 5 and 10 μs) than during the plateau (at 11 and 50 μs), when it becomes negligible. All in all, the maximum value of the conduction current is orders of magnitude larger than the maximum value of the displacement current.

The distribution of the current density, conduction and displacement components, as a function of time, is shown in the region close to the membrane (a $100\,\text{nm} \times 100\,\text{nm}^2$) in Figure 2(b). In the membrane region, the displacement component of the current density [middle line Figure 2(b)] is relevant (~2,000 A/m^2) during pulse rise time and negligible in the pulse plateau.

3.2 Influence of the nanoparticle

In this section, the results related to different NPs with different positions along the cell membrane for the two different pulse rise times are reported.

The analyzed NPs are positioned close to the cell membrane facing the positive electrode and along the radial direction at 45° with respect to the normal direction to the positive electrode [Figure 1(d)]. The electric field strength is evaluated in the ROI shown as a red rectangle in Figure 1(d), and along the line L_c passing through the cell interior, cell exterior and the NP core. Both horizontal and vertical oriented NPs are considered.

Considering the trapezoidal voltage pulse in Figure 1(b), the electric field strength is investigated for different time instants, i.e. in the middle of rise time, $t_r/2$ (being t_r the rise time of the applied pulse) for which the derivative of the displacement vector is not null, and in the middle of the pulse plateau, $t_p/2$ (i.e. 55 μs), for which a direct current phase is established. The electric field strength is evaluated on the L_c line for the time instant $t_r/2$ and $t_p/2$.

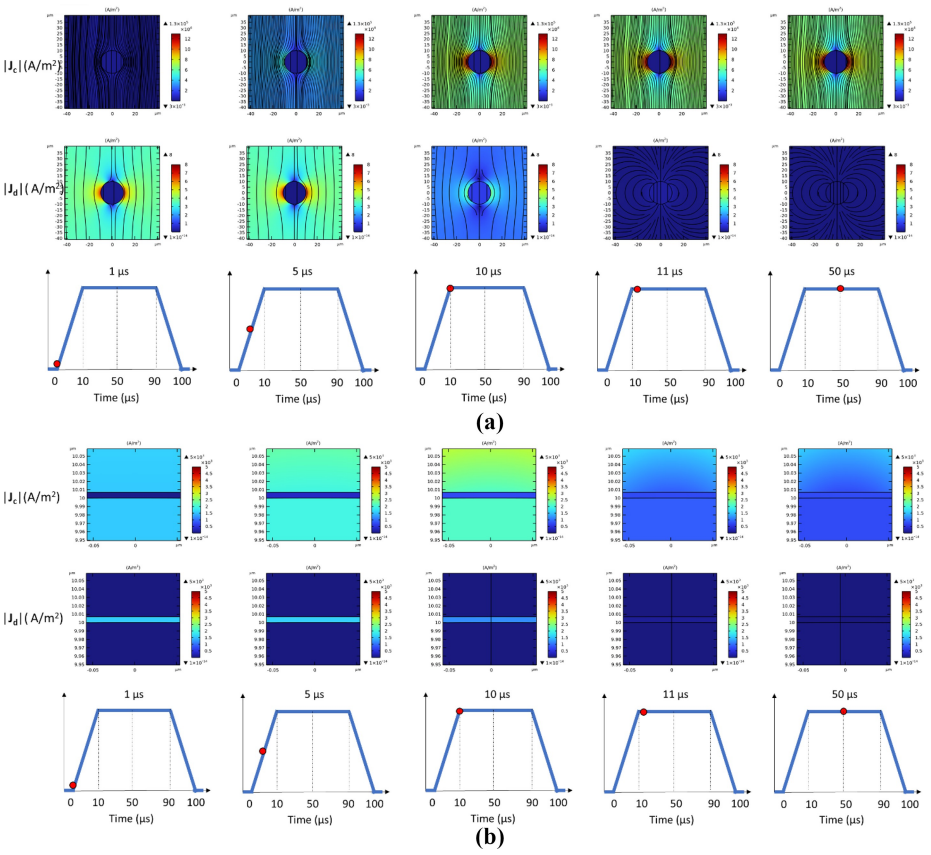

Figure 2. Evaluation of the conduction current (upper line), $|J_c|$, and displacement current density (middle line), $|J_d|$, at 1, 5, 10, 11 and 50 µs in (a) the entire domain and (b) on the membrane (the rectangular strip is the membrane)

Source: Authors' own work

3.3 Horizontal-oriented nanoparticle

The colormap of the electric field strength evaluated at 55 µs, i.e. in the plateau zone of the pulse, without the NP (Figure 3) is compared to the one with the two different NPs, made of gold and dielectric material, respectively. The field is evaluated considering the pulse with 1 µs of rise time and the NP in position P_0 in Figure 1(d). Figure 4 shows differences in the electric field distribution due to the NP positioned close to the cell membrane. These variations highlight the impact of NPs on local electric field distribution in electroporation conditions.

In the case of the gold NP, the most prominent feature is the electric field strength approaching zero within the NP core, a good conductive material, evidenced by the deep blue region observed in Figure 4(a). The NP acts as a shield due to the rapid redistribution of free charges. Whereas, for a dielectric NP, the electric field approaches the maximum value [Figure 4(b)]. Consequently, the electric field is forced to bypass the

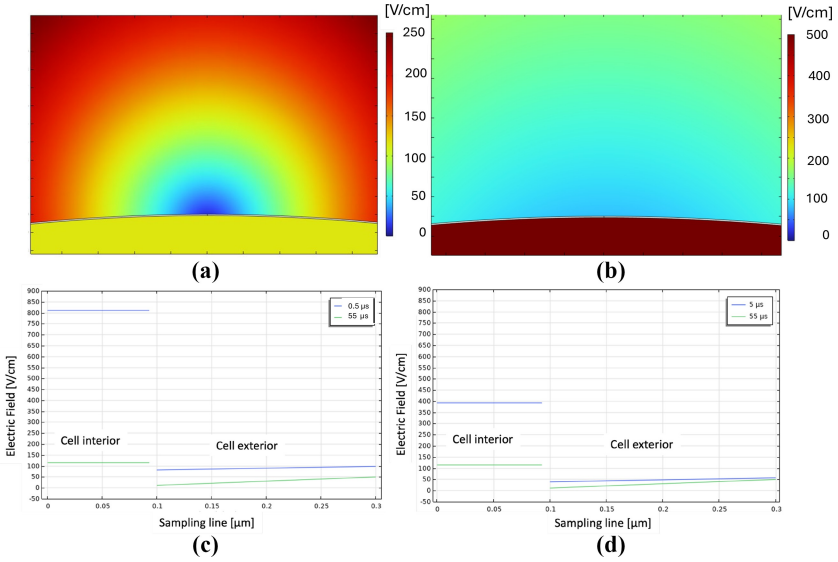

Figure 3. Electric field strength for the case without NP position P_0 in Figure 1(d) at (a) 55 μs and (b) at $t_r/2 = 0.5$ μs, considering a pulse with a rise time of 1 μs. Electric field along L_c for (e) and (f) gold and (g) and (h) dielectric nanoparticle for a pulse rise time of (e)–(g) 1 μs and (f)–(h) 10 μs

Source: Authors' own work

NP, leading to a high electric field depicted by the intense red and orange regions primarily around the NP edge, increasing the electric field at NP extremities with respect to the case without NP. Then, the dielectric NP modifies the electric field strength close to the membrane.

The dielectric NP core shows a significant enhancement of the electric field [red color, Figure 4(a)] because the NP electric permittivity and conductivity are lower than those of the surrounding medium. High electric field magnitudes are also visible immediately surrounding the NP, particularly at its upper surface. The electric field directly close to the cell membrane appears to have a different distribution compared to the gold NP and without NP cases. Then, both NPs locally modify the electric field in different ways.

Figure 4(e)–(h) shows the different behavior of the electric field strength in proximity to the NP: the electric field at $t_p/2$, when the transient effect of the derivative of the displacement field is null. As expected for conductive materials, the electric field inside the gold NP core is null [Figure 4(e) and (f)]. However, in the surrounding media close to the cell membrane, the electric field is enhanced only at the NP edge. Instead, considering a dielectric NP during pulse rise time, the electric field is enhanced in the proximity of the cell membrane [Figure 4(g) and (h)]. Moreover, it is to be noted that the red color in the color scale corresponds to a double electric field strength with respect to that obtained for the direct current conduction case, in Figure 4(a). Consequently, during the pulse rise time, the electric field in proximity to the membrane is higher than that in the direct conduction case. This suggests an enhancement of the electric field strength in the presence of the NP during pulse rise time, due to the derivative of the displacement field.

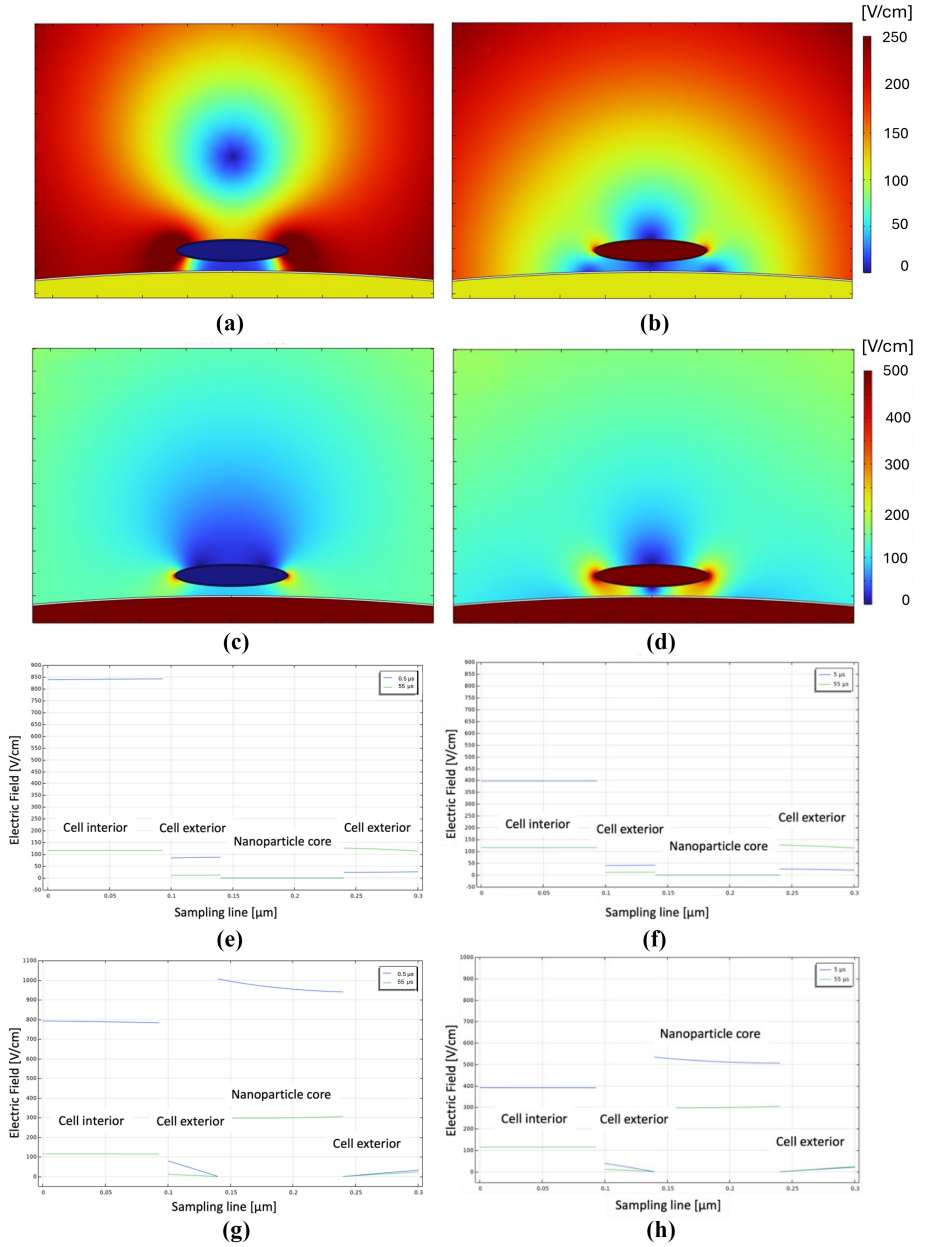

Figure 4. Color plot of the electric field strength for (a)–(c) gold and (b)–(d) dielectric nanoparticle horizontally-oriented in position P_0 in Figure 1(d) at (a)–(c) 55 μs and (b)–(d) at $t_r/2$, considering a pulse with a rise time of 1 μs. Electric field along L_c for (e) and (f) gold and (g) and (h) dielectric nanoparticle for a pulse rise time of (e)–(g) 1 μs and (f)–(h) 10 μs

Source: Authors' own work

In summary, at $t_r/2$ with a 1 μs rise time, both NPs modify the distribution of the electric field around the NP. Gold NP enhances the electric field at the edge around its conductive body by redirecting the electric field lines, leading to a shielded interior. In contrast, the dielectric NP allows the field to permeate and concentrate within its volume, resulting in a different electric field distribution. An enhancement occurs both within and at the boundaries of the NP itself. The gold and dielectric NPs provide a different mechanism for influencing the electric field near the cell membrane during the initial phase of the pulse.

Figure 4(e) and (f), shows the electric field strength along the line L_c for the horizontal-oriented gold NP in P_0 [Figure 1(d)] considering a sampling time equal to $t_r/2$ (0.5 and 5 μs) for rise time 1 μs and 10 μs, respectively. The highest electric field occurs inside the cell during the pulse rise time. On the contrary, in the region outside the cell, the electric field strength at 55 μs is higher than the one at $t_r/2$. The electric field gap between the interior and exterior of the cell membrane, as expected, is comparable at 55 μs, in the middle of the pulse plateau for both the rise time [Figure 4(e) and (f), 1 μs and 10 μs rise-time]. Nevertheless, the electric field gap between the internal and external sides of the membrane is larger during the transient than at the plateau and larger for the lower rise time, 1 μs.

Figure 4(f) shows the case of gold NP for which a pulse with a rise time of 10 μs is applied. The electric field strength at $t_r/2$, i.e. 5 μs for a 10 μs pulse rise time, is higher than at 55 μs for the cell interior and between the NP and the cell membrane. Specifically, the electric field strength within the cell is around 120 V/cm at 55 μs, independently of the rise time, whereas during pulse rise time, the electric field strength is approximately 840 V/cm for 1 μs and 400 V/cm for 10 μs. In the region between the cell membrane and NP, the electric field strength is lower and under 100 V/cm in the case of a 1 μs pulse rise time and under 50 V/cm for a 10 μs rise time. This suggests that a faster rise time leads to a more intense electric field build-up across the cell and its vicinity, which is a critical aspect for electroporation.

Comparing the results considering the rise-time 1 μs or 10 μs [Figure 4(g) and (h),] in the case of dielectric NPs horizontally oriented, evident differences in the electric field strength are observed at $t_r/2$ and 55 μs. In the case of dielectric NP, the electric field in the cell interior at 55 μs assumes the same value as in the case of gold NP. Therefore, the NP does not influence the electric field strength in the cell interior when the direct current phase is established. The difference with the gold NP is inside the NP core, which experiences the highest electric field strength and reaches 1,000 V/cm during the 1 μs pulse rise time, and in the region between the cell membrane and the NP, where the electric field decreases from the cell membrane moving toward the NP. In the region outside the NP toward the electrode, the electric field is influenced by the type of NP, and it is lower in the case of dielectric NP.

3.4 Vertically-oriented nanoparticle

The comparison of the color plots representing the electric field strength at 55 μs, considering a voltage pulse with a 1 μs rise time for a gold and a dielectric NP in vertically-oriented position P_0, is shown in Figure 5.

Considering the vertically-oriented gold NP [Figure 5(a)], and the direct current case, i.e. at 55 μs, the electric field at the NP edge is lower with respect to the case without the NP, and has a different distribution. In particular, the gold NP reduces the size of the area with a low electric field value. Instead, considering the vertically-oriented dielectric NP, the electric field strength in the ROI is lower than that in the case without NP. Moreover, the electric field is less affected with respect to the horizontal NP case.

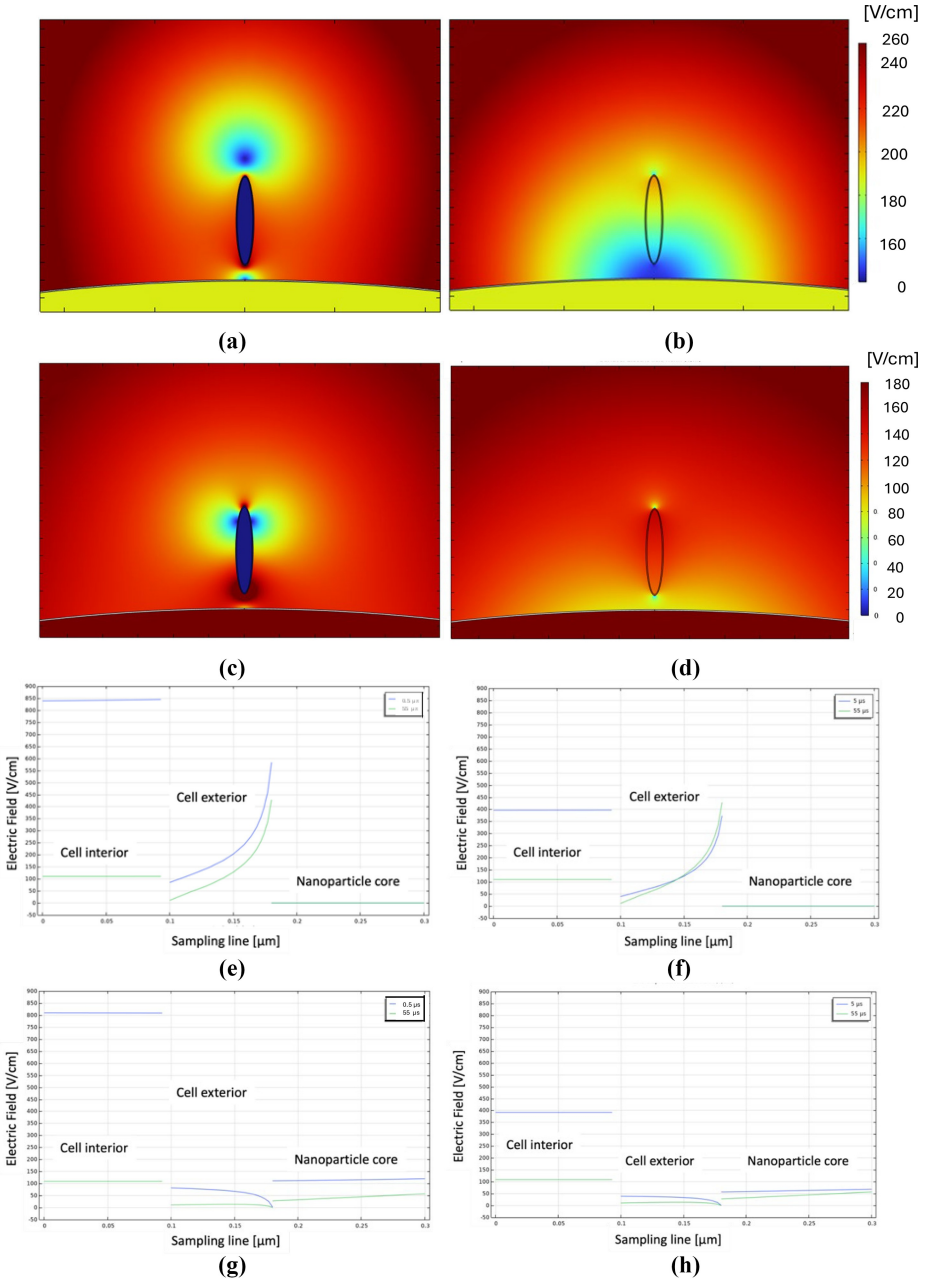

Figure 5. Electric field strength for (a)–(c) gold and (b)–(d) dielectric nanoparticle vertically-oriented in position P_0 at (a) and (b) 55 µs and at (c) and (d) tr/2 considering a pulse with a rise time of 1 μs. Electric field along L_c for (e) and (f) gold and (g) and (h) dielectric nanoparticle for a pulse rise time of (e)–(g) 1 μs and (f)–(h) 10 μs

Source: Authors' own work

Considering the electric field strength around the vertically-oriented NP during the rise time of 1 μs pulse, the gold NP enhances the electric field between the NP and the cell membrane, while in the case of a dielectric NP, it is lower [Figure 5(c) and (d)].

Considering a vertically-oriented NP [Figure 5(e) and (f)] and a rise time of 1 or 10 μs, respectively, there are differences in the electric field strength (V/cm) evaluated along the line L_c at 0.5 or 5 μs, depending on the pulse rise time.

Figure 5(e) and (f), shows the electric field strength along the line L_c for a gold NP. The electric field inside the cell is the same found for the horizontally-oriented NP considering the same time instants, i.e. $t_r/2$ and 55 μs. At $t_r/2$, the electric field strength for the voltage pulse with 1 μs rise time increases moving from the cell to the NP. As in the case of horizontally-oriented NP, the electric field at the $t_r/2$ assumes a higher electric field value considering the shorter rise time, i.e. 1 μs, with respect to the longer rise time, i.e. 10 μs. In the NP core, there are no significant differences for the rise times considered. In contrast, with a 10 μs rise time, the electric field strength at $t_r/2$, in the region between the cell and NP, is superposed to the one evaluated at 55 μs, i.e. in the direct current conduction phase.

In the case of dielectric NP [Figure 5(g) and (h)], the electric field strength along the line L_c has a different behavior with respect to the case of gold NP. In the NP core, the electric field is not null, and in the region between the cell and NP, the electric field decreases close to the NP.

The electric field inside the cell is lower in the presence of a dielectric NP with respect to the gold NP, specifically, the difference is equal to 50 V/cm. This difference is more pronounced and reaches higher values with a faster voltage pulse rise time, suggesting that pulse dynamics are critical for the local field in the presence of gold or dielectric NPs.

3.5 45°-oriented nanoparticle

Figure 6 shows the color plots representing the electric field strength at 55 μs [Figure 6(a) and (b)], and at $t_r/2$ [Figure 6(c) and (d)], considering a pulse with a 1 μs rise time for the NP in position P_{45} [Figure 1(d)]. The behavior of the electric field is similar to the one of the horizontal NP with a lower electric field intensity.

Considering the gold and dielectric NP in position P_{45} at 55 μs, the electric field strength sampled on the line L_c in the region between cell membrane and NP, the electric field strength is lower for the gold NP than for the dielectric NP [Figure 6(e) and (f)].

In the literature (Guo *et al.*, 2022), some simulation results without NPs related to the electric field distribution close to the cell are reported and they are comparable with the obtained distribution. Moreover, the distribution of electric field, and an enhanced electric field, in the presence of a prolate NP is comparable to the one found by Lekner (Lekner, 2014).

Considering this analysis, it can be evidenced that the gold NP increases the electric field inside the cell during pulse rise time (Figure 4). These phenomena do not occur with dielectric NPs. Considering the different orientations of NP, it can be observed that the horizontally oriented NP improves the electric field strength in proximity of NP extremities with respect to the same NP vertically oriented during pulse plateau [Figure 4(e) and (f), for gold and Figure 4(g) and (h), for dielectric NP horizontal-oriented and Figure 6(e) and (f), for gold and Figure 6(g) and (h), for dielectric NP vertical-oriented]. Instead of then it occurs in the plateau part of the pulse, during pulse rise-time the electric field strength is enhanced in the area of NP extremities if compared to the no-NP case (Figure 3). Moreover, the electric field shows an evident difference at the extremity of the NP if gold [Figure 4(a)] or dielectric material is considered [Figure 4(c)].

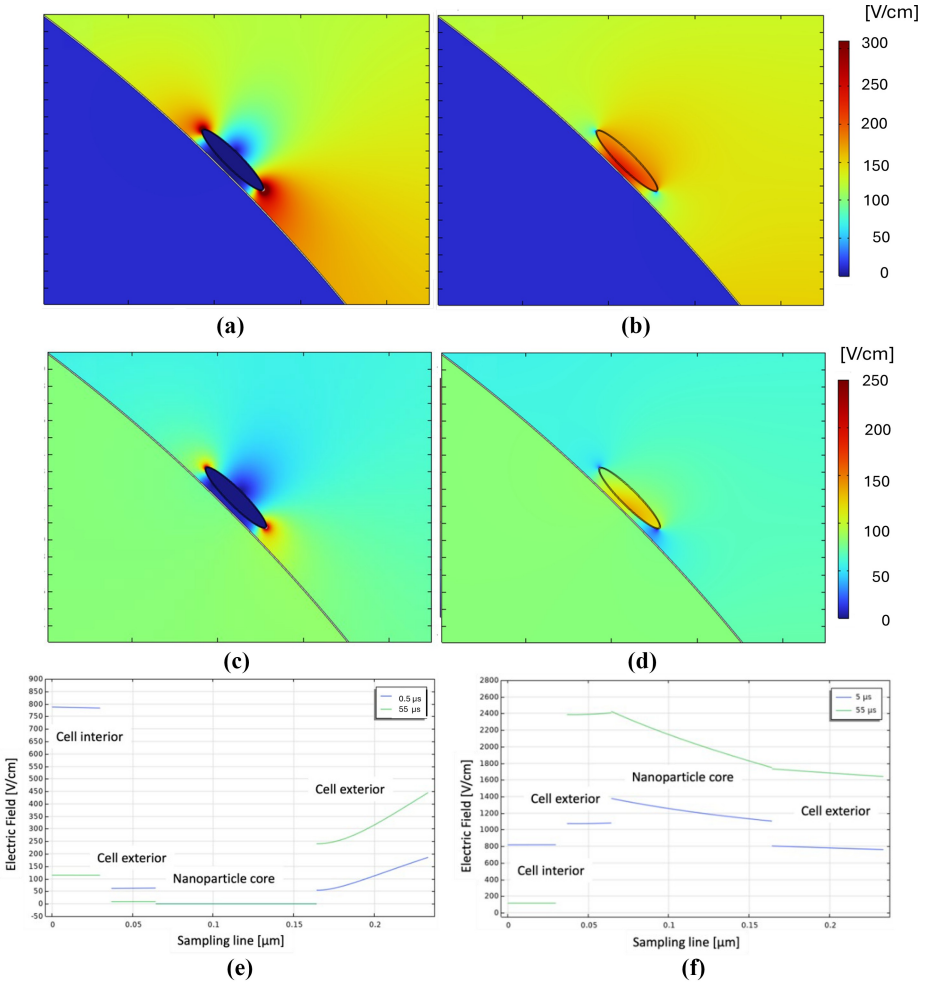

Figure 6. Electric field strength for (a)–(c) gold and (b)–(d) dielectric nanoparticle in position P_{45} at (a) and (b) 55µs and at (c) and (d) tr/2 considering a pulse with a rise time of 1 μs

Source: Authors' own work

4. Conclusion

The obtained results show how the electric field is modified in a region close to the cell membrane, a nonconductive region, in the presence of a gold and dielectric NP with different orientations. From the results, it appears that the NP orientation influences the electric field distribution in the region of analysis. In the simulated conditions, the gold or dielectric NPs used show opposite effects for the same applied voltage pulses. Moreover, considering the derivative of electric displacement in the computational model allows the proper calculation of the difference in the electric field distribution due to the presence of the NP during the pulse rise time. In the present work, it was evidenced that the pulse rise time can modify the transmembrane potential. Then, the proposed model is able to quantify the effect of

displacement current during the pulse rise time in a more complete model since the pulse rise time is studied. In fact, the faster the pulse rise time, the higher the electric field gap is between the internal and external parts of the cell. In future work, different cells will be investigated, taking into account all their electrical properties.

References

AZoM (2026), "Properties: silica – silicon dioxide (SiO2)", available at: www.azom.com/properties.aspx?ArticleID=1114 (accessed 4 October 2025).

Bertacchini, C. (2017), "Cliniporator: medical electroporation of tumors", in Miklavcic, D. (Ed.), *Handbook of Electroporation*, Springer International Publishing, Cham, pp. 1-36.

Campana, L.G., Bullo, M., Di Barba, P., Dughiero, F., Forzan, M., Mognaschi, M.E., Sgarbossa, P., Tosi, A.L., Bernardis, A. and Sieni, E. (2018), "Effect of tissue inhomogeneity in soft tissue sarcomas: from real cases to numerical and experimental models", *Technology in Cancer Research and Treatment*, Vol. 17, p. 153303381878969.

Chiaramello, E., Fiocchi, S., Bonato, M., Gallucci, S., Benini, M. and Parazzini, M. (2021a), "Use of nanoparticles as nanoelectrodes in contact-less cell membrane permeabilization by time-varying magnetic field: a computational study", *Applied Sciences*, Vol. 11 No. 23, p. 11121.

Chiaramello, E., Fiocchi, S., Bonato, M., Gallucci, S., Benini, M. and Parazzini, M. (2021b), "Cell transmembrane potential in contactless permeabilization by time-varying magnetic fields", *Computers in Biology and Medicine*, Vol. 135, p. 104587.

Corovic, S., Lackovic, I., Sustaric, P., Sustar, T., Rodic, T. and Miklavcic, D. (2013), "Modeling of electric field distribution in tissues during electroporation", *BioMedical Engineering OnLine*, Vol. 12 No. 1, p. 16.

Denzi, A., Strigari, L., Di Filippo, F., Botti, C., Di Filippo, S., Perracchio, L., Ronchetti, M., Cadossi, R. and Liberti, M. (2015), "Modeling the positioning of single needle electrodes for the treatment of breast cancer in a clinical case", *BioMedical Engineering OnLine*, Vol. 14 No. S3, p. S1.

Ferry, D.K. and Rode, D.L. (2025), "Physical and electrical properties of silica", *Applied Physics Reviews*, Vol. 12 No. 1, p. 011304.

Gauthier, M.M. (Ed.) (1995), *Engineered Materials Handbook Desk Edition*, ASM International.

Gehl, J. (2003), "Electroporation: theory and methods, perspectives for drug delivery, gene therapy and research", *Acta Physiologica Scandinavica*, Vol. 177 No. 4, pp. 437-447.

Gehl, J., Sersa, G., Matthiessen, L.W., Muir, T., Soden, D., Occhini, A., Quaglino, P., Curatolo, P., Campana, L.G., Kunte, C., Clover, A.J.P., Bertino, G., Farricha, V., Odili, J., Dahlstrom, K., Benazzo, M. and Mir, L.M. (2018), "Updated standard operating procedures for electrochemotherapy of cutaneous tumours and skin metastases", *Acta Oncologica*, Vol. 57 No. 7, pp. 874-882, doi: 10.1080/0284186X.2018.1454602.

Ghorbel, A., Mir, L.M. and García-Sánchez, T. (2019), "Conductive nanoparticles improve cell electropermeabilization", *Nanotechnology*, Vol. 30 No. 49, p. 495101.

Goldberg, E., Suárez, C., Alfonso, M., Marchese, J., Soba, A. and Marshall, G. (2018), "Cell membrane electroporation modeling: a multiphysics approach", *Bioelectrochemistry*, Vol. 124, pp. 28-39.

Guo, F., Gou, X., Sun, J., Hong, J. and Zhang, Y. (2024), "Modeling methods in overlapping electroporation treatments: pulse number effects on tissue conductivity and ablation area", *Electrochimica Acta*, Vol. 503, p. 144883.

Guo, F., Qian, K., Li, X. and Deng, H. (2022), "Simulation study of cell transmembrane potential and electroporation induced by time-varying magnetic fields", *Innovative Food Science and Emerging Technologies*, Vol. 81, p. 103117.

Haus, H.A. and Melcher, J.R. (1989), *Electromagnetic Fields and Energy*, Prentice Hall, Englewood Cliffs, NJ.

IGEA (2026), available at: www.igeamedical.com/ (accessed 15 April 2014).

Ivorra, A., Villemejane, J. and Mir, L. (2010), "Electrical modeling of the influence of medium conductivity on electroporation", *Physical Chemistry Chemical Physics*, Vol. 12 No. 34, pp. 10055-10064.

Kranjc, M. and Miklavčič, D. (2016), "Electric field distribution and electroporation threshold", in Miklavcic, D. (Ed.), *Handbook of Electroporation*, Springer International Publishing, Cham, pp. 1-17.

Krassowska, W. and Filev, P.D. (2007), "Modeling electroporation in a single cell", *Biophysical Journal*, Vol. 92 No. 2, pp. 404-417.

Labeed, F.H., Coley, H.M. and Hughes, M.P. (2006), "Differences in the biophysical properties of membrane and cytoplasm of apoptotic cells revealed using dielectrophoresis", *Biochimica et Biophysica Acta (BBA) - General Subjects*, Vol. 1760 No. 6, pp. 922-929.

Lamberti, P., Romeo, S., Sannino, A., Zeni, L. and Zeni, O. (2015), "The role of pulse repetition rate in nsPEF-induced electroporation: a biological and numerical investigation", *IEEE Transactions on Biomedical Engineering*, Vol. 62 No. 9, pp. 2234-2243.

Lamberti, P., Tucci, V., Romeo, S., Sannino, A., Scarfì, M.R. and Zeni, O. (2013), "nsPEF-induced effects on cell membranes: use of electrophysical model to optimize experimental design", *IEEE Transactions on Dielectrics and Electrical Insulation*, Vol. 20 No. 4, pp. 1231-1238.

Lekner, J. (2014), "Electroporation in cancer therapy without insertion of electrodes", *Physics in Medicine and Biology*, Vol. 59 No. 20, pp. 6031-6042.

Meunier, Gerard (2008), "The finite element method for electromagnetic modeling", *ISTE Ltd*, Wiley.

Mir, L.M. (2001), "Therapeutic perspectives of in vivo cell electropermeabilization", *Bioelectrochemistry*, Vol. 53 No. 1, pp. 1-10.

Mir, L.M. (2006), "Bases and rationale of the electrochemotherapy", *European Journal of Cancer Supplements*, Vol. 4 No. 11, pp. 38-44.

Mir, L.M., Gehl, J., Sersa, G., Collins, C.G., Garbay, J.-R., Billard, V., Geertsen, P.F., Rudolf, Z., O'Sullivan, G.C. and Marty, M. (2006), "Standard operating procedures of the electrochemotherapy: Instructions for the use of bleomycin or cisplatin administered either systemically or locally and electric pulses delivered by the CliniporatorTM by means of invasive or non-invasive electrodes", *European Journal of Cancer Supplements*, Vol. 4 No. 11, pp. 14-25.

Pavlin, M., Kandušer, M., Reberšek, M., Pucihar, G., Hart, F.X., Magjarevićcacute, R. and Miklavčič, D. (2005), "Effect of cell electroporation on the conductivity of a cell suspension", *Biophysical Journal*, Vol. 88 No. 6, pp. 4378-4390.

Poignard, C., Silve, A. and Wegner, L. (2016), "Different approaches used in modeling of cell membrane electroporation", edited by Miklavcic, D. *Handbook of Electroporation*, Springer International Publishing, Cham.

Polajžer, T., Kranjc, M., Kralj, S., Caf, M., Romih, R., Hudoklin, S., Rocca, F. and Miklavčič, D. (2025), "Limited efficacy of Nanoparticle-Assisted electroporation for membrane permeabilization and gene electrotransfer", *Pharmaceutics*, Vol. 17 No. 8, p. 964.

Pucihar, G., Kotnik, T., Kandušer, M. and Miklavčič, D. (2001), "The influence of medium conductivity on electropermeabilization and survival of cells in vitro", *Bioelectrochemistry*, Vol. 54 No. 2, pp. 107-115.

Sel, D., Cukjati, D., Batiuskaite, D., Slivnik, T., Mir, L.M. and Miklavcic, D. (2005), "Sequential finite element model of tissue electropermeabilization", *IEEE Transactions on Biomedical Engineering*, Vol. 52 No. 5, pp. 816-827.

Sieni, E., Nemec, S., Lamberti, P., Romeo, S., Sgarbossa, P., Forzan, M., Golzio, M., Rols, M.P., Kolosnjaj-Tabi, J. and Kralj, S. (2023), "Electric field distribution in cell aggregates in presence of nanostructures under electroporation pulses", *2023 IEEE Nanotechnology Materials and Devices Conference (NMDC)*, *IEEE*, *Paestum*, *Italy*, pp. 174-179.

Wang, K., Zhao, Y., Chen, D., Fan, B., Lu, Y., Chen, L., Long, R., Wang, J. and Chen, J. (2017), "Specific membrane capacitance, cytoplasm conductivity and instantaneous young's modulus of single tumour cells", *Scientific Data*, Vol. 4 No. 1, p. 170015.

Ye, H., Cotic, M., Kang, E.E., Fehlings, M.G. and Carlen, P.L. (2010), "Transmembrane potential induced on the internal organelle by a time-varying magnetic field: a model study", *Journal of NeuroEngineering and Rehabilitation*, Vol. 7 No. 1, p. 12.

Zhao, Y., Zhao, X.T., Chen, D.Y., Luo, Y.N., Jiang, M., Wei, C., Long, R., Yue, W.T., Wang, J.B. and Chen, J. (2014), "Tumor cell characterization and classification based on cellular specific membrane capacitance and cytoplasm conductivity", *Biosensors and Bioelectronics*, Vol. 57, pp. 245-253.

Zu, Y., Huang, S., Liao, W.-C., Lu, Y. and Wang, S. (2014), "Gold nanoparticles enhanced electroporation for mammalian cell transfection", *Journal of Biomedical Nanotechnology*, Vol. 10 No. 6, pp. 982-992.

Zudans, I., Agarwal, A., Orwar, O. and Weber, S.G. (2007), "Numerical calculations of single-cell electroporation with an electrolyte-filled capillary", *Biophysical Journal*, Vol. 92 No. 10, pp. 3696-3705.

Corresponding author
Elisabetta Sieni can be contacted at: elisabetta.sieni@uninsubria.it

COMPEL - The international journal for computation and mathematics in electrical and electronic engineering